Journal Pre-proof

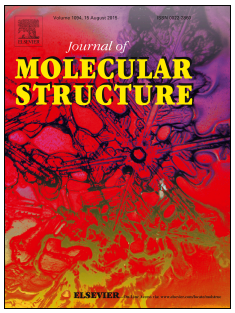

Molecular and supramolecular structures of self-assembled Cu(II) and Co(II) complexes with 4,4'-[6-(3,5-dimethyl-1*H*-pyrazol-1-yl)-1,3,5-triazine-2,4-diyl]dimorpholine ligand

Saied M. Soliman, Matti Haukka, Hessa H. Al-Rasheed, Ayman El-Faham

PII: S0022-2860(20)30909-1

DOI: https://doi.org/10.1016/j.molstruc.2020.128584

Reference: MOLSTR 128584

To appear in: *Journal of Molecular Structure*

Received Date: 23 April 2020

Revised Date: 30 May 2020

Accepted Date: 1 June 2020

Please cite this article as: S.M. Soliman, M. Haukka, H.H. Al-Rasheed, A. El-Faham, Molecular and supramolecular structures of self-assembled Cu(II) and Co(II) complexes with 4,4'-[6-(3,5-dimethyl-1*H*-pyrazol-1-yl)-1,3,5-triazine-2,4-diyl]dimorpholine ligand, *Journal of Molecular Structure* (2020), doi: https://doi.org/10.1016/j.molstruc.2020.128584.

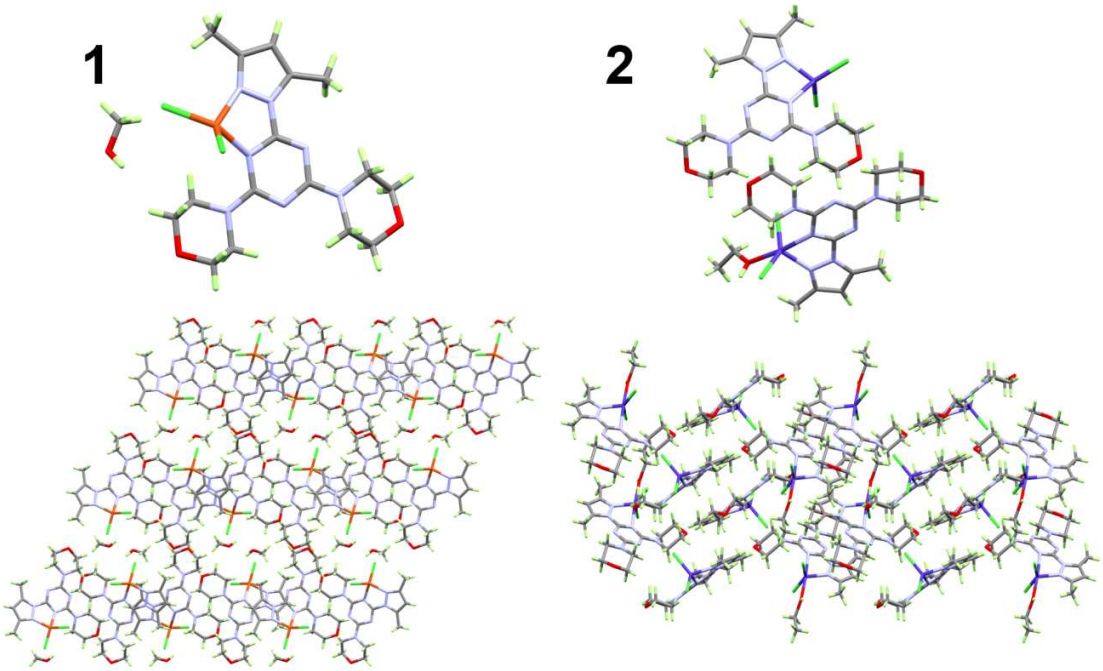

Molecular and supramolecular structures of self-assembled Cu(II) and Co(II) complexes with 4,4'-[6-(3,5-dimethyl-1*H*-pyrazol-1-yl)-1,3,5-triazine-2,4-diyl]dimorpholine ligand

Saied M. Soliman[1]*, Matti Haukka[2], Hessa H. Al-Rasheed [3], Ayman El-Faham[1,3]

[1] Department of Chemistry, Faculty of Science, Alexandria University, P.O. Box 426, Ibrahimia, Alexandria 21321, Egypt.

[2] Department of Chemistry, University of Jyväskylä, P.O. Box 35, FI-40014 Jyväskylä, Finland.

[3] Department of Chemistry, College of Science, King Saud University, P. O. Box 2455, Riyadh 11451, Saudi Arabia.

***** Correspondence: Saied M. Soliman: saied1soliman@yahoo.com.

Abstract

The molecular and supramolecular structures of [Cu(PTM)Cl_2]*0.75MeOH (**1**), [Co(PTM)Cl_2]; (**2A**) and [Co(PTM)Cl_2(EtOH)]; (**2B**) complexes, where **PTM** is 4,4'-[6-(3,5-dimethyl-1*H*-pyrazol-1-yl)-1,3,5-triazine-2,4-diyl]dimorpholine, were presented. In complexes **1** and **2A**, the Cu(II) and Co(II) are tetra-coordinated with a distorted tetrahedral coordination environment. In case of complex **2B**, an additional ethanol molecule is found coordinated with Co(II) leading to a highly distorted penta-coordinated Co(II) complex. In all cases, the **PTM** ligand is acting as a bidentate *NN*-chelate. Hirshfeld surface analysis indicated the importance of H…H (49.0-55.1%), Cl…H (18.8-20.5%) and O…H (8.3-9.9%) contacts in the molecular packing. The electron transferences from the ligand units to the central metal atom as well as the spin density distribution were discussed based on DFT calculations. The presence of coordinated ethanol molecule in **2B** weakened the Co-N and Co-Cl interactions compared to **2A**. Using atoms in molecules topology analysis, the coordinate bonds between metal (Co or Cu) and donor atoms (N, O, Cl) belong to closed shell interactions with weak covalent characters.

Keywords: Pyrazolyl-*s*-triazine; Co(II); Cu(II); NBO; Spin density; Hirshfeld

1. Introduction

Supramolecular compounds attracted the interest of researchers due to the tremendous progress in their applications in different fields [1-8]. Many new functional compounds having wonderful supramolecular architectures were constructed from self-assembly of functional ligand and metal ion. Such methodology allowed the small building blocks to arrange itself in the three dimensions by the way that maximize the intermolecular interactions among them [9-11]. The self-arrangements of the small molecular units in solid state is controlled by many directional forces such as coordination interactions, hydrogen bonding, π-π stacking, C-H… π interactions and others [12].

On other hand, copper and cobalt complexes have many interesting applications in numerous fields [13]. For example, Ghosh *et al*. reported the synthesis of a series of CO_2-promoted polymeric copper(II) coordination complexes [13c]. The reported complexes showed interesting semiconducting property over a wide temperature range [13c]. In addition, cobalt complexes with the 2-(2-hydroxybenzylideneamino)phenol as *ONO*-donor ligand have been reported with promising antibacterial and anticancer activities [13a]. Recently, Ramezani *et al*.[13b], reported the synthesis and characterization of two Co(II) complexes with heterocyclic Schiff-base ligands based on the reaction of *p*-chlorobenzaldehyde and *p*-hydroxybenzaldehyde with 8-(4- chlorophenyl)-3-alkyl-3*H*-imidazo[4',5':3,4]benzo[1,2-*c*]isoxazol-5-amines. These complexes exhibited interesting fluorescent properties [13b].

Neutral *NNN*-pincer ligands attracted the attention of many researchers in the field of coordination chemistry and showed remarkable success in building interesting coordination compounds having interesting applications in the field of catalysis [14]. *NNN*-pincer ligands with pyridine central moieties and unsaturated nitrogen donor moieties at 2 and 6 positions have been studied extensively. Replacement of the pyridine core with *s*-triazine ring has a great impact on the ligand coordination behavior and the intermolecular contacts involved in building the supramolecular architecture of the resulting complexes [15-18]. In our previous studies we mainly focused on the coordination chemistry as well as the antimicrobial activity of *bis*-pyrazolyl-*s*-triazine tridentate pincer ligand (**BPT; Fig. 1**). It was found that, the self-assembly of this ligand with different metal(II) salts produced mononuclear penta-, hexa- and hepta-coordinated

metal complexes. The supramolecular architectures of these complexes were constructed mainly by hydrogen bonds and anion-π stacking interactions between the *s*-triazine ring π-system and the counter anion [15-18]. Replacement of the methoxy group and one pyrazolyl ring in **BPT** by two morpholine rings (**PTM)** as shown in **Fig. 1** reduced the ligand coordination behavior to bidentate leading to interesting mononuclear and penta-nuclear Ag(I) complexes [19]. Herein we used the same mild conditions of self-assembly to synthesize the corresponding Co(II) and Cu(II) complexes of this functional ligand. Their molecular and supramolecular structures were investigated using X-ray single crystal diffraction combined with Hirshfeld surface analysis as well as DFT calculations.

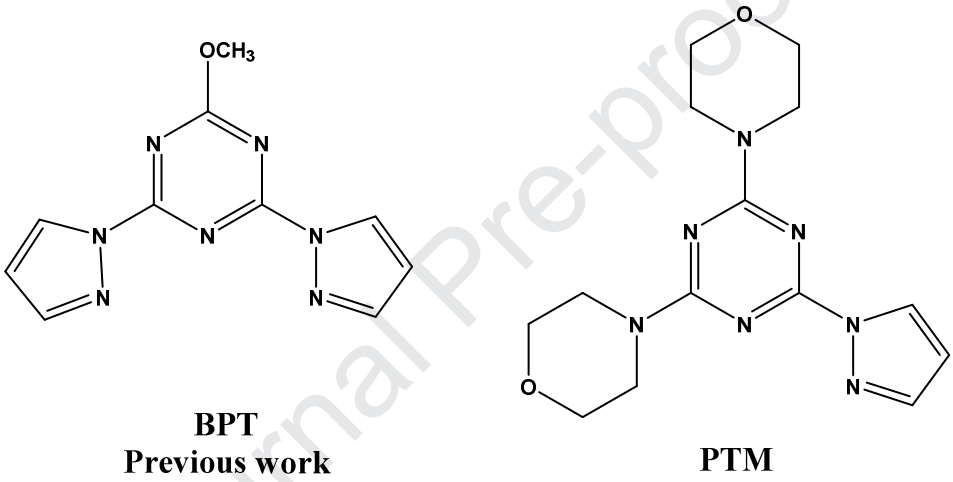

Fig. 1 Structure of *bis*-pyrazolyl-*s*-triazine (**BPT**) and **PTM** ligands.

2. Experimental

2.1. Materials and physical measurements

Chemicals and solvents were purchased from Sigma-Aldrich Company. The CHN analyses were determined using Perkin-Elmer 2400 elemental analyzer. The NMR spectra of **PTM** were recorded on a JEOL spectrometer (400 MHz) in $CDCl_3$ solvent.

2.2. Syntheses

2.2.1. 4,4'-(6-(3,5-dimethyl-1*H*-pyrazol-1-yl)-1,3,5-triazine-2,4-diyl)dimorpholine, PTM ligand

The ligand **PTM** was prepared following the reported method in literature [20-22]. Details regarding the preparation and characterization of **PTM** ligand were given in supplementary data.

2.2.2. Synthesis of Cu(II)-PTM complex (1)

A 10 mL methanolic solution of $CuCl_2 \cdot 2H_2O$ (0.170 g, 1 mmol) was mixed with **PTM** (0.345 mg, 1 mmol) solution in 10 mL methanol (**Scheme 1**). The resulting solution was left for slow evaporation, bronze needles of $[Cu(PTM)Cl_2]$*0.75MeOH (**1**) was obtained after 3 days.

Yield 89 %; Anal. Calc. for complex (**1**) $C_{16.75}H_{26}Cl_2CuN_7O_{2.75}$: C, 39.93; H, 5.20; N, 19.46%. Found: C, 39.75; H, 5.17; N, 19.29%.

2.2.3. Synthesis of Co(II)-PTM complex (2)

A 10 mL ethanolic solution of $CoCl_2 \cdot 6H_2O$ (0.238 g, 1 mmol) was mixed with **PTM** (0.345 mg, 1 mmol) solution in 10 mL ethanol (**Scheme 1**). Purple block crystals of $[Co(PTM)Cl_2][Co(PTM)Cl_2(EtOH)]$, (**2**) was obtained after slow evaporation for 2 days.

Yield 85%: Anal. Calc. for complex (**2**) $C_{34}H_{52}Cl_4Co_2N_{14}O_5$: C, 40.98; H, 5.26; N, 19.68%. Found: C, 40.81; H, 5.30; N, 19.50%.

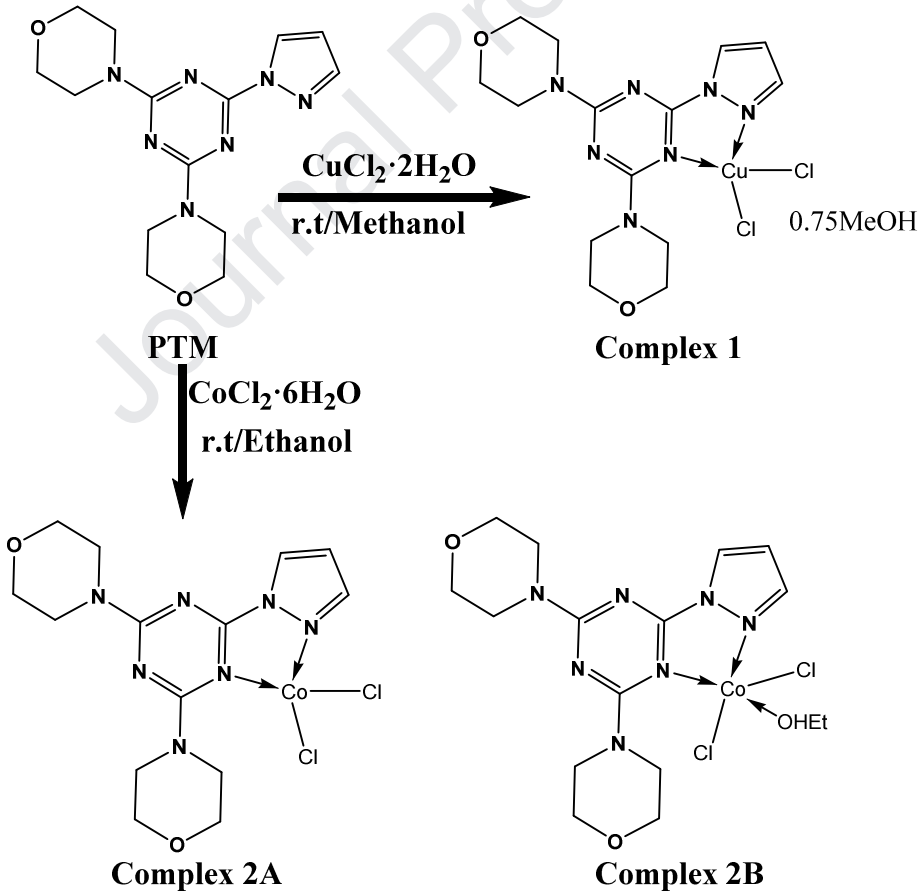

Scheme 1 Syntheses of complexes **1** and **2**.

2.4. X-Ray structure determinations

The X-ray diffraction data of **1** and **2** were collected on a Bruker Kappa Apex II diffractometer using Mo Kα radiation. The Bruker *SAINT* [23a] software was used for cell refinements and data reductions. The structures were solved by intrinsic phasing method using the *SHELXT* software [23b]. A semi-empirical absorption correction based on equivalent reflections (*SADABS* [23c]) was applied to all data. Structural refinements were carried out using *SHELXL* software [23b]. Further crystallographic details about structure refinements were described in Supplementary data and **Table 1**. Crystal Explorer 17.5 program was used for doing Hirshfeld calculations [24].

Table 1 Crystal data of complexes 1 and 2.

	1	**2**
Empirical formula	$C_{16.75}H_{26}Cl_2CuN_7O_{2.75}$	$C_{34}H_{52}Cl_4Co_2N_{14}O_5$
Fw	503.88	996.55
Temp (K)	293(2)	108(2)
λ(Å)	0.71073	0.71073
Cryst. Syst.	Monoclinic	Triclinic
Space group	C2/c	P-1
a (Å)	26.7629(5)	7.688(3)
b (Å)	7.42190(10)	13.757(6)
c (Å)	23.7102(4)	21.102(9)
α(deg)	90	81.276(9)
β (deg)	117.5020(5)	79.919(9)
γ (deg)	90	74.429(9)
V (Å^3)	4177.38(12)	2103.8(16)
Z	8	2
ρ_{calc} (Mg/m^3)	1.602	1.573
μ(Mo Kα) (mm^{-1})	1.335	1.102
No. reflns.	14985	34456
Unique reflns.	3819	7664
GOOF (F^2)	1.040	1.041
R_{int}	0.0216	0.0416
R1 ($I \geq 2\sigma$)	0.0403	0.0890
wR2 ($I \geq 2\sigma$)	0.1048	0.2168
CCDC	1998255	1998256

3. DFT calculations

Using NBO 3.1 program [25a] embedded in Gaussian 09 software [25b, c], the natural charges at the ligand groups and metal ion were calculated using MPW1PW91/TZVP method using the Cartesian coordinate of the X-ray structure for the studied complexes. For the Co(II) complexes, the calculations were performed considering the high and low spin states and the results were discussed based on the most stable state. In addition, Multiwfn [26a] program was used to compute the atoms in molecules (AIM) topological parameters [26b].

4. Results and discussion

4.1. X-ray structure description of complex 1

The X-ray structure of [Cu(PTM)Cl_2]*0.75MeOH (**1**) is shown in **Figure 2**. Complex **1** crystallized in the monoclinic crystal system and C2/c space group, and Z=8 with one molecule per asymmetric unit. The structure of **1** comprised one Cu(II) coordinating the bidentate **PTM** ligand as *NN*-chelate with almost equidistant Cu1-N1 and Cu-N6 bonds (2.000(2) and 2.005(2) Å, respectively), and two chloride anions with Cu1-Cl1 and Cu1-Cl2 distances of 2.1783(9) and 2.2284(8) Å, respectively. The structure contains heavily disordered methanol molecules as a crystal solvent found close to the symmetry elements with total occupancy of 0.75. Hence the molecular structure of **1** is [Cu(PTM)Cl_2]*0.75MeOH. The bite angle of the **PTM** ligand is 80.54(9)º for the N1-Cu1-N6 while the Cl1-Cu1-Cl6 angle is 105.44(4)º (**Table 2**). The copper atom is out of the mean planes of the *s*-triazine and pyrazole moieties by 0.759 and 0.459 Å, respectively. The angle between the mean planes of the two rings is 7.1º indicating the presence of some twist between the *s*-triazine and pyrazole moieties. The continuous shape measurements (CSHM) of the CuN_2Cl_2 coordination sphere are 8.5 and 12.1 compared to the perfect tetrahedral (Td) and square planar (SqP) geometries, respectively [28]. The values are relatively high indicating an intermediate structure between the Td and SqP geometries.

Table 2 Selected bond lengths [Å] and angles [°] for 1.

Bond	Distance	Bonds	angle
Cu1-N1	2.000(2)	N1-Cu1-N6	80.54(9)
Cu1-N6	2.005(2)	N1-Cu1-Cl1	102.56(7)
Cu1-Cl1	2.1783(9)	N6-Cu1-Cl1	144.31(8)
Cu1-Cl2	2.2284(8)	N1-Cu1-Cl2	134.75(7)
		N6-Cu1-Cl2	95.96(7)
		Cl1-Cu1-Cl2	105.44(4)

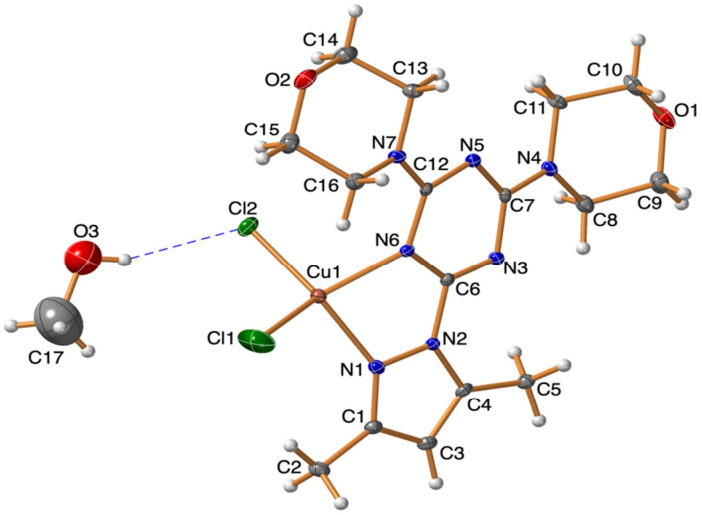

Fig. 2 The anisotropic displacements plot (ADP) at 50% probability of complex **1**. Only one of the disordered methanol solvent molecules is shown. H-bond: O3-H3A$^{\#1}$: 0.83 Å, H3A···Cl2$^{\#1}$: 2.54 Å, O3··· Cl2$^{\#1}$: 3.339(1) Å, O3-H3A···Cl2$^{\#1}$: 160.5º (equivalent position #1: -x, 1+y, ½-z).

The structure of **1** contained heavily disordered methanol as solvent of crystallization. In **Fig. 3**, the solvent was completely omitted from the packing diagram to reveal solvent channels along the crystallographic *b*-axis (**Fig. 3A**). The neighboring complex units are interacting with a series of weak H-bond-interactions (**Fig. S1**; Supplementary data) leading to stacking of metal complexes (**Fig. 3b**). Despite the stacking, there are no significant π-π-interactions between the organic ligand units of **1**.

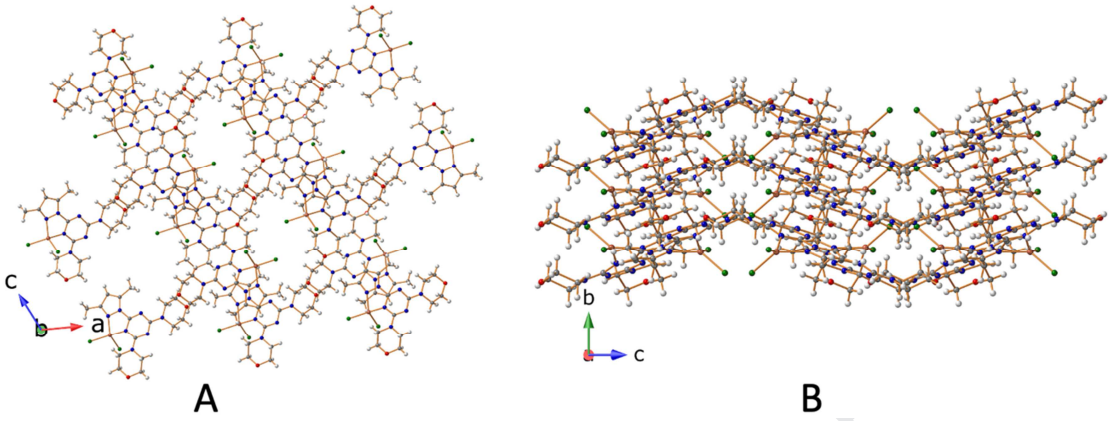

Fig. 3 Packing of **1** along the crystallographic *b*-axis (A) and *a*-axis (B).

4.2. X-ray structure description of complex 2

The asymmetric unit of **2** consists of the two independent neutral complex units, [Co(PTM)Cl_2]; (**2A**) and [Co(PTM)Cl_2(EtOH)]; (**2B**), in which the Co(II) has different coordination environments (**Fig. 4**). The structure of [Co(PTM)Cl_2] is similar to that in complex **1**. The Co(II) is coordinated with one **PTM** molecule as a bidentate *NN*-chelate where the Co1B-N1B and Co1B-N5B distances are 2.016(6) and 2.103(5) Å, respectively. The two Co-N bonds are not equivalents and are slightly longer than the corresponding Cu-N bonds in **1**. The coordination sphere of Co1B is completed by two Co-Cl bonds which are also slightly longer than the Cu-Cl bonds in **1**. The Co1B-Cl1B and Co1B-Cl2B bond distances are 2.192(3) and 2.241(2) Å, respectively. The bite angle of the **PTM** ligand is 79.6(2)º and the Cl1B-Co1B-Cl2B angle is 119.48(13)º (**Table 3**). In this complex, the CSHM values for the CoN_2Cl_2 are 4.46 and 21.27 compared to Td and SqP geometries, respectively. The former value is closer to zero indicating a distorted tetrahedral CoN_2Cl_2 coordination environment rather than a square planar, which is expected for a tetra-coordinated Co(II) complexes.

In the second complex unit, [Co(PTM)Cl_2(EtOH)], the Co(II) is penta-coordinated with one **PTM** ligand (Co1-N1: 2.033(6) Å and Co1-N6: 2.288(6)Å), two chloride ions (Co1-Cl1: 2.320(2) Å and Co1-Cl2: 2.270(2) Å) and one weakly bonded ethanol molecule (Co1-O3: 2.225(7) Å). The bite angle of the **PTM** ligand is less (75.3(2)º) than that in [Co(PTM)Cl_2] while the Cl1-Co1-Cl2 (144.52(9)º) is larger than that in [Co(PTM)Cl_2]. These variations could be probably attributed to the presence of coordinated ethanol

molecule which increases the steric hinder around the Co(II) as a consequence of increasing the coordination number of Co(II) from 4 in [Co(PTM)Cl_2] to 5 in [Co(PTM)Cl_2(EtOH)]. The coordination geometry of the CoN_2Cl_2O sphere was described using the τ_5 criterion reported by Addison [29]. The O3-Co1-N6 angle (β) of 174.5(2)º and Cl2-Co1-Cl1 angle (α) of 144.52(9)º, and a $\tau_5 = \left\{\frac{(\beta-\alpha)}{60}\right\}$ value of 0.50 revealed an intermediate structure between the distorted square pyramid and trigonal bipyramid coordination geometry. In addition, the Co1 and Co1B occurred out of the plane of the *s*-triazine and pyrazole rings. The Co1B atom is out of the mean planes of the *s*-triazine and pyrazole moieties by 0.781 and 0.241 Å, respectively. The corresponding values for the Co1 atom are 0.898 and 0.214 Å, respectively. Also, the twist angles of the two rings are 10.37 and 13.28 º for Co1B and Co1 units, respectively.

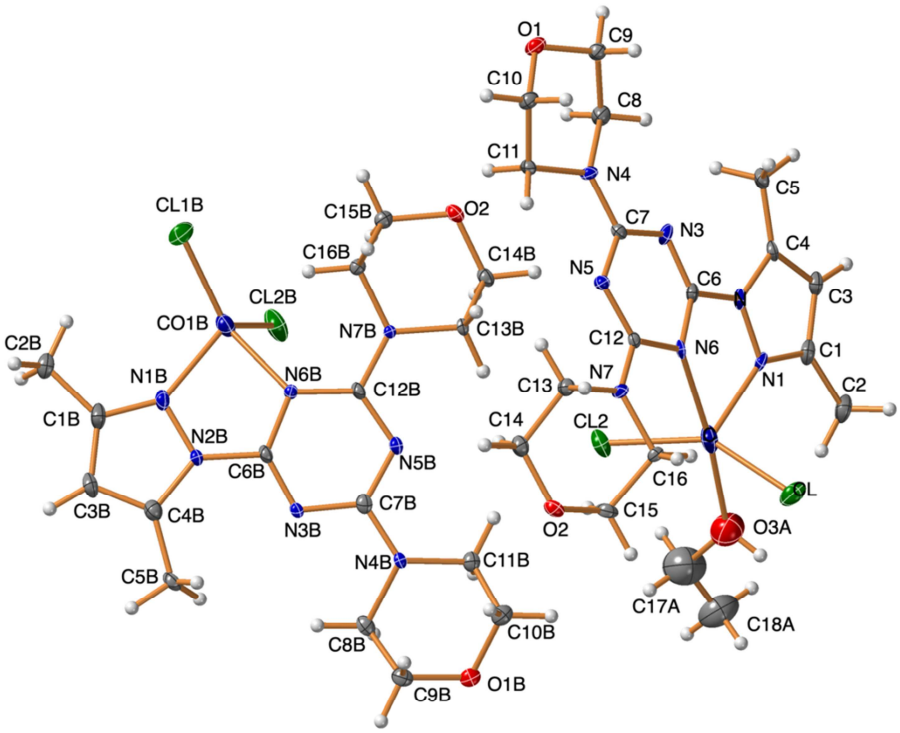

Fig. 4 The anisotropic displacements plot (ADP) at 50% probability of complex **2**. One of the morpholine moiety in the four-coordinated complex and the ethanol ligand in the five-coordinated complex were disordered over two sites. Only the dominating components are shown in this figure for better clarity.

Table 3 Selected bond lengths [Å] and angles [°] for 2.

bond	Distance	Bonds	Angle
		[Co(PTM)Cl_2]	
Co1B-N1B	2.016(6)	N1B-Co1B-N6B	79.6(2)
Co1B-N6B	2.103(5)	N1B-Co1B-Cl1B	107.21(17)
Co1B-Cl1B	2.192(3)	N6B-Co1B-Cl1B	129.32(19)
Co1B-Cl2B	2.241(2)	N1B-Co1B-Cl2B	119.03(17)
		N6B-Co1B-Cl2B	97.00(16)
		Cl1B-Co1B-Cl2B	119.48(13)
		[Co(PTM)Cl_2(EtOH)]	
Co1-N1	2.033(6)	N1-Co1-O3	109.0(3)
Co1-N6	2.288(6)	N1-Co1-Cl2	114.13(16)
Co1-Cl1	2.320(2)	O3-Co1-Cl2	88.5(2)
Co1-Cl2	2.270(2)	N1-Co1-N6	75.3(2)
Co1-O3	2.225(7)	O3-Co1-N6	174.5(2)
		C2-Co1-N(6	86.53(14)
		N1-Co1-Cl1	101.25(16)
		O3-Co1-Cl1	77.1(2)
		Cl2-Co1-Cl1	144.52(9)
		N6-Co1-Cl1	105.73(16)

Also in complex **2**, the molecules are packed (**Fig. 5**) with two crystallogarphically slightly different stacks compared to **1**. The aromatic rings are somewhat closer than in **1** allowing some weak π-π and C-H…π interactions. The shortest C…C and C…N contacts are C4B···C6B$^{\#2}$: 3.393(12) Å (#1: -1-x,-1-y, #2: -x,-y,1-z) and N6···C5$^{\#1}$: 3.237(14) Å. In addition, the channels in **2** are running through the structure along crystallographic *a*-direction (**Fig. 5**) and the channels are not filled with solvent but are occupied by the coordinated ethanol molecules. Further details about the packing of the complex molecular units are shown in **Figs. S2** and **S3** (Supplementary data).

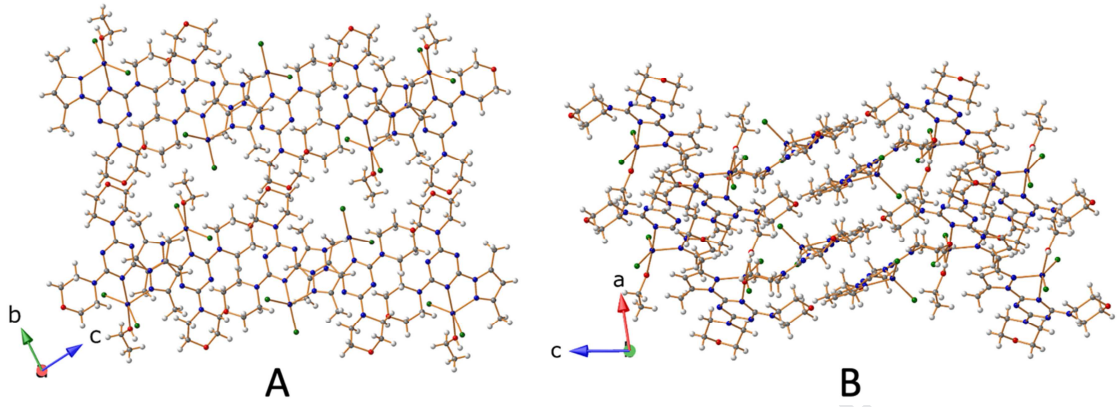

Fig. 5 Packing of **2** along the crystallographic *a*- (A) and *b*-directions (B).

4.3. Analysis of molecular packing

Intermolecular interactions play very important role in the stability of crystalline materials. Different contacts in the crystal structure of complexes **1** and **2** were analyzed using Hirshfeld calculations and the resulting Hirshfeld surfaces are shown in **Figs. S4** and **S5** (Supplementary data). The percentages of the possible intermolecular contacts in both complexes are shown in **Fig. 6**. The H…H interactions are the most common which shared in the packing by 50.5, 49.0 and 55.1% for **1**, **2A** and **2B**, respectively. It is clear from the decomposed d_{norm} maps shown in **Figs. 7-9** that the H…H interactions are strong contrary to the structurally related pincer complexes [15-18]. Representative examples for the most significant H…H, Cl…H and O…H contacts are shown in the same figure where all showed the characteristic red spots for short contacts. The percentages of the Cl…H contacts are 16.2, 20.5 and 18.8% for **1**, **2A** and **2B**, respectively while the O…H contacts showed less contributions of 9.7, 8.3 and 9.9%, respectively. Analysis of d_{norm} and shape index maps indicated the less significance of the π-π (3.9-5.2%) and C-H…π (4.2-4.9%) interactions in the molecular packing of the studied complexes.

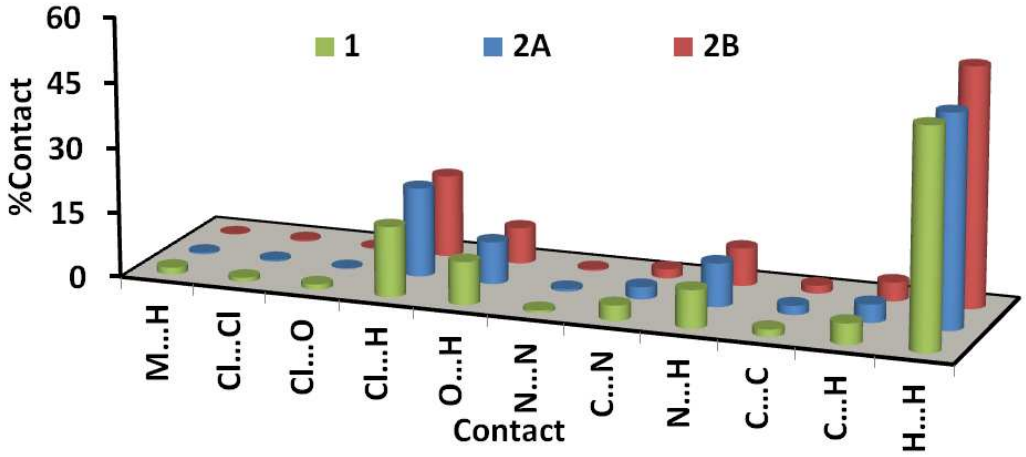

Fig. 6 Possible contacts in complexes **1**, **2A** and **2B**.

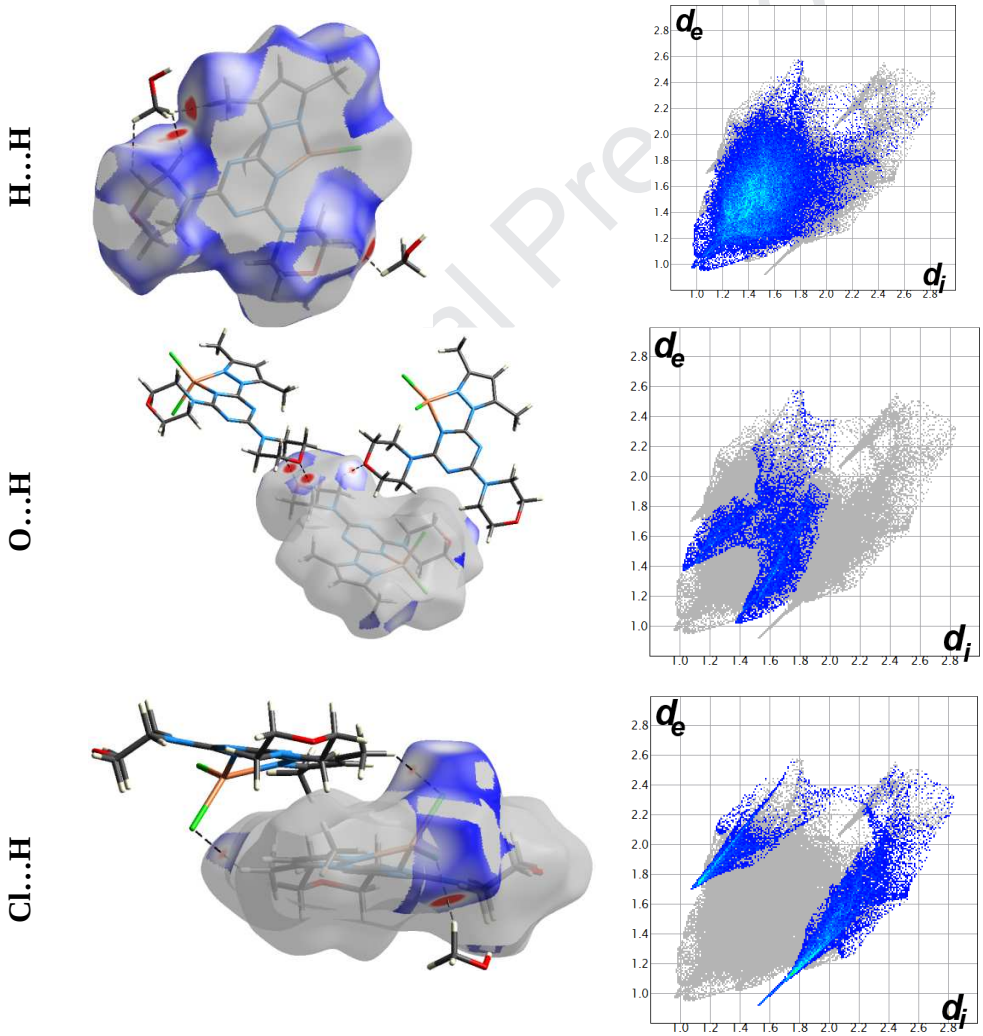

Fig. 7 Hirshfeld surface analysis of H…H, O…H and Cl…H contacts in **1**.

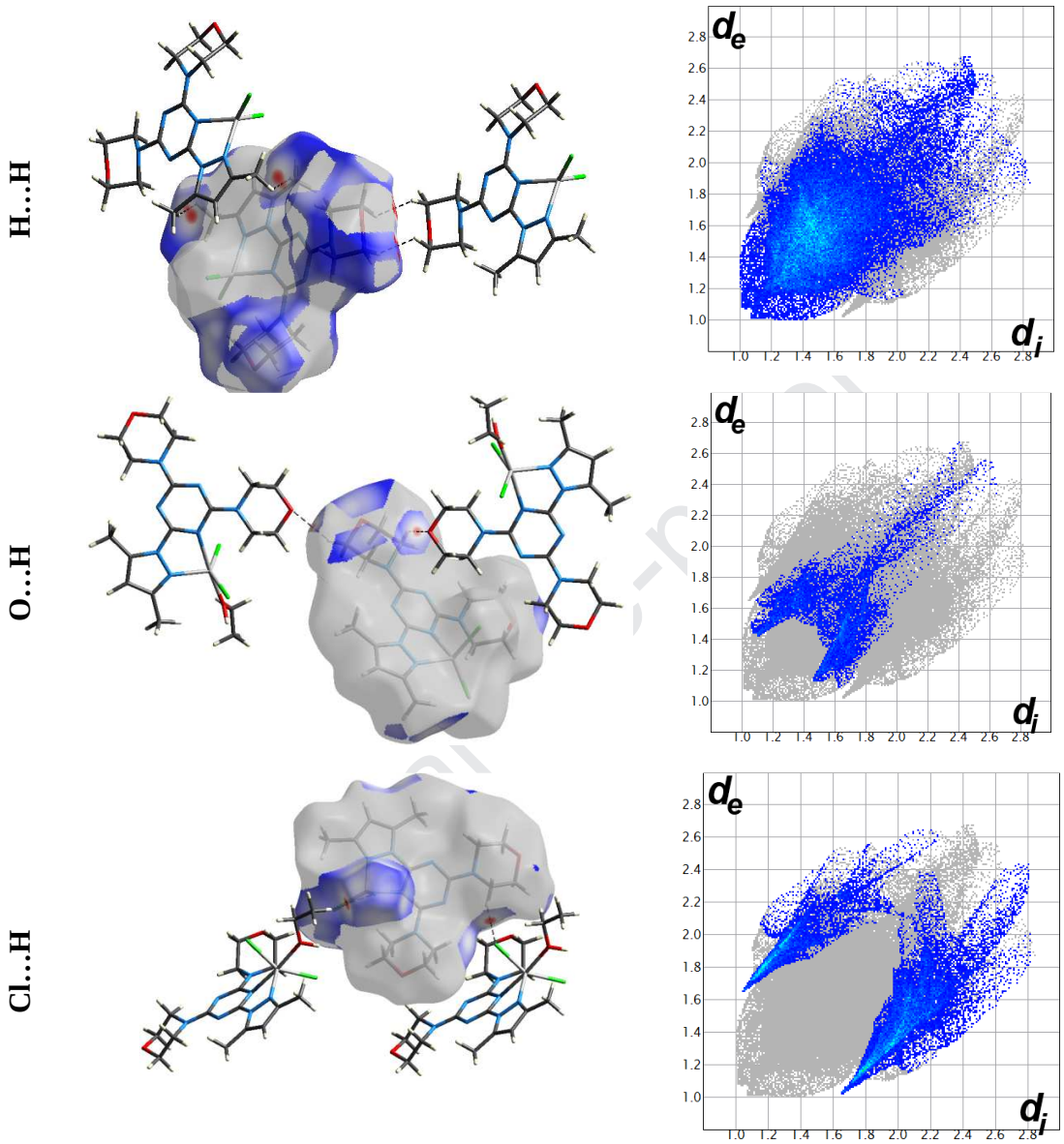

Fig. 8 Hirshfeld surface analysis of H…H, O…H and Cl…H contacts in **2A**.

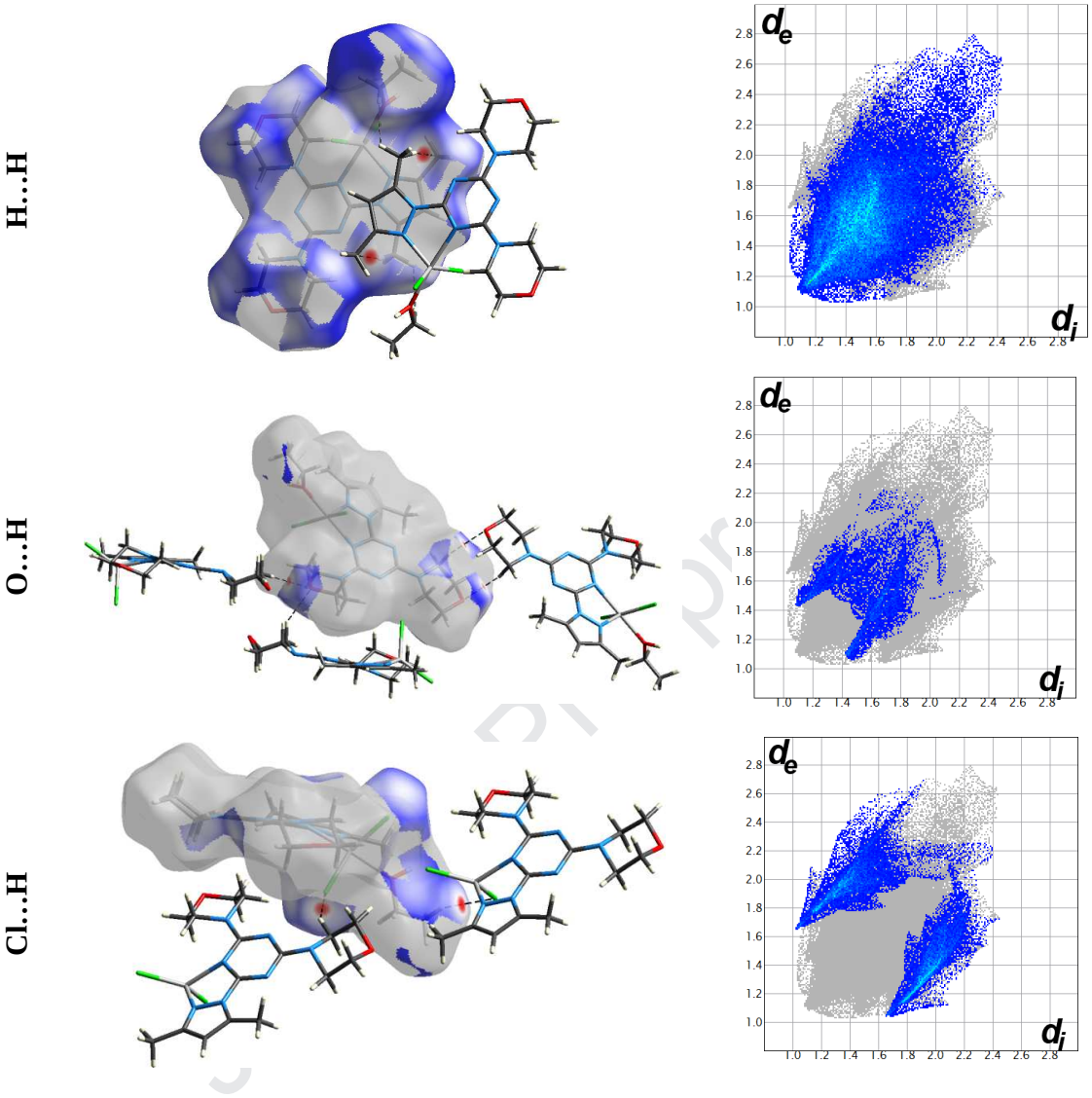

Fig. 9 Hirshfeld surface analysis of H…H, O…H and Cl…H contacts in **2B**.

4.4. DFT studies

The total energy of the high and low spin states of [Co(PTM)Cl_2]; (**2A**) and [Co(PTM)Cl_2(EtOH)]; (**2B**) are calculated using MPW1PW91/TZVP method. The total energies of the high spin state of **2A** and **2B** are -2171582.021 and -2268862.237 kcal/mole, respectively. The corresponding values for the low spin state are -2171543.253 and -2268834.409 kcal/mole, respectively. As a result, the high spin state is more stable for both complexes than the low spin states by 38.77 and 27.83 kcal/mole, respectively. The organic ligand (**PTM**) has net charges of 0.3958, 0.3586 and 0.300 for

1, **2A** and **2B**, respectively (**Table 4**). It is the minimum in case of the penta-coordinated Co(II) complex. The presence of two chloride ions and one ethanol molecule coordinating the Co(II) significantly weaken its interaction with the **PTM** organic ligand probably due to both of the steric and electronic factors. The presence of more donor groups around Co(II) decreases its positive charge density leading to weaker interactions with the **PTM** ligand. As a result of these electron transferences from the ligand groups to the divalent metal ion, the charge densities at the central metal atom are reduced to 0.659, 0.756 and 0.838, for **1**, **2A** and **2B**, respectively.

Table 4 Natural charges of metal center and ligand groups.

Atom/Group	**1**	**2A**	**2B**
Co1/Cu1	0.6590	0.7560	0.8380
Cl1	0.4814	0.4515	0.3740
Cl2	0.4639	0.4339	0.3950
PTM	0.3958	0.3586	0.3000
EtOH			0.0930

Also, the atom spin density of donor atoms and central metal ion are listed in **Table 5**. High spin Co(II) has a spin density of 3.0 e. This value is reduced to 2.734 and 2.751 e due to its interaction with ligand donor atoms. The N, O and Cl donor atoms have positive spin density similar to the central metal ion indicating a transfer of the spin density *via* spin delocalization mechanism rather than the spin polarization one. Also, the spin density of copper center in complex **1** is changed to 0.594 e instead of 1.0 e due to spin delocalization from the central metal to donor atoms coordinating it. Graphical presentation of the spin density plot for the three complexes is given in **Fig. S7** (Supplementary data).

Table 5 Spin density of the donor atoms and the central metal ion in complexes **1**, **2A** and **2B**.

Atom	**1**	**2A**	**2B**
Cu/Co	0.5941	2.7342	2.7505
Cl1	0.1470	0.0993	0.0853
Cl2	0.1501	0.0965	0.0867
$\mathbf{N_{triaz.}}$	0.0472	0.0162	0.0242
$\mathbf{N_{pyraz.}}$	0.0498	0.0122	0.0140
O3			0.0084

4.5. Atoms in molecules (AIM) analysis

The topological parameters computed in the framework of AIM theory were used to assign the nature and strength of coordination interactions [31-38]. These parameters are listed in **Table 6**. Generally, the electron density (ρ(r)) is considered as a good indicator on bond strength. For complex **1**, the two Cu-N interactions have close ρ(r) values where Cu-N(pyrazole) has slightly higher ρ(r) value than Cu-N(triazine). The same trend is found in the two Co(II) complex units of **2**. Interestingly, the presence of coordinated ethanol molecule in **2B** weakens the Co-N and Co-Cl interactions compared to **2A**. The most clear difference occurred for the Co-N(triazine) with ρ(r) value of 0.045 a.u. in **2B** compared to 0.088 a.u in **2A**. Similarly, the Co-Cl interactions have slightly less ρ(r) values (0.055-0.062 a.u.) in **2B** compared to **2A** (0.066-0.074 a.u.). In contrast, the strength of the Cu-N(pyrazole) is affected little by the presence of coordinated ethanol molecule. The calculated interaction energies ($E_{int.}$) for the Co-N and Co-Cl bonds are in good agreement with these observations. It is clear that all the studied coordination interactions presented in **Table 6** have ρ(r) less than 0.1 a.u indicating mainly closed shell coordination interactions. In addition, the small negative total energy density (H(r)) and the potential to kinetic energy density ratio (V(r)/G(r)) more than one are good indicators on the weak covalent characters of these interactions.

Table 5 The AIM topological parameters for the studied coordination interactions[a].

Bond	ρ(r)	G(r)	V(r)	E_{int}	H(r)	V(r)/G(r)
			1			
Cu1-N1	0.071	0.094	-0.101	31.841	-0.007	1.079
Cu1-N6	0.065	0.094	-0.098	30.762	-0.004	1.043
Cu1-Cl1	0.058	0.086	-0.089	27.833	-0.003	1.035
Cu1-Cl2	0.050	0.072	-0.071	22.415	0.000	0.994
			2A			
Co1B-N1B	0.088	0.125	-0.148	46.306	-0.023	1.184
Co1B-N6B	0.070	0.089	-0.101	31.558	-0.012	1.131
Cu1-Cl1	0.074	0.100	-0.117	36.698	-0.017	1.173
Cu1-Cl2	0.066	0.088	-0.099	31.142	-0.011	1.128
			2B			
Co1-N1	0.083	0.120	-0.140	43.908	-0.020	1.168
Co1-N6	0.045	0.051	-0.052	16.366	-0.001	1.028
Co1-Cl1	0.055	0.070	-0.075	23.514	-0.005	1.075
Co1-Cl2	0.062	0.081	-0.089	28.049	-0.009	1.107
Co1-O3	0.043	0.063	-0.066	20.564	-0.003	1.046

[a] **All in A.U. except $E_{int.}$ in kcal/mol**

Conclusion

Two complexes of 4,4'-[6-(3,5-dimethyl-1*H*-pyrazol-1-yl)-1,3,5-triazine-2,4-diyl]dimorpholine (**PTM**) ligand with Cu(II) and Co(II) were synthesized using self-assembly in water-alcohol mixture at room temperature. The structure of complexes **1** and **2** comprised the $[Cu(PTM)Cl_2]$*0.75MeOH (**1**), and $[Co(PTM)Cl_2]$; (**2A**) and $[Co(PTM)Cl_2(EtOH)]$; (**2B**) molecular units, respectively as revealed by single crystal X-ray diffraction. Their supramolecular structure aspects were analyzed employing Hirshfeld surface analysis of molecular packing. The spin density of coordinated metal ion was transferred to the donor atoms *via* spin delocalization mechanism. Based on Addison τ_5 criterion, the coordination geometry of **2B** is highly distorted with an intermediate structure between the square pyramidal and trigonal bipyramidal configurations. The nature and strength of the coordination interactions were analyzed using atoms in molecules topology analysis.

Acknowledgements

The authors would like to extend their sincere appreciation to the Deanship of Scientific Research at King Saud University for providing funding to the research group no. RG - 1441-365, Saudi Arabia.

Conflicts of interest

The authors declare that they have no known competing financial interests or personal relationships that could have appeared to influence the work reported in this paper.

References

[1] K.S. Mali, N. Pearce, S.D. De Feyter, N.R. Champness, Frontiers of supramolecular chemistry at solid surfaces, Chem. Soc. Rev., 46 (2017) 2520-2542.

[2] I.V. Kolesnichenko, E.V. Anslyn, Practical applications of supramolecular chemistry, Chem. Soc. Rev., 46 (2017) 2385-2390.

[3] L. Qin, J. Zheng, S.L. Xiao, X.H. Zheng, G.H. Cui, A new supramolecular net constructed with 2D (4,4) layer subunits displaying unique 4-connected msw/*P*42/*nnm* topology: Structure, fluorescence and catalytic properties, Inorg. Chem. Commun., 34 (2013) 71-74.

[4] J. He, J.X. Zhang, G.P. Tan, Y.G. Yin, D. Zhang, M.H. Hu, Second Ligand-Directed Assembly of Photoluminescent Zn(II) Coordination Frameworks, Cryst. Growth Des., 7 (2007) 1508-1513.

[5] S.K. Das, M.K. Bhunia, S.M. Motin, S. Dutta, A. Bhaumik, Highly porous Co(II)-salicylate metal–organic framework: synthesis, characterization and magnetic properties, Dalton Trans., 40 (2011) 2932-2939.

[6] E.V. Alexandrov, V.A. Blatov, A.V. Kochetkov, D.M. Proserpio, Underlying nets in three-periodic coordination polymers: topology, taxonomy and prediction from a computer-aided analysis of the Cambridge Structural Database, Cryst. Eng. Comm., 13 (2011) 3947-3958.

[7] S. Kitagawa, R. Kitaura, S.I. Noro, Functional Porous Coordination Polymers, Angew. Chem. Int. Ed., 43 (2004) 2334-2375.

[8] S. Hu, K.H. He, M.H. Zeng, H.H. Zou, Y.M. Jiang, Crystalline-State Guest-Exchange and Gas-Adsorption Phenomenon for a “Soft” Supramolecular Porous Framework Stacking by a Rigid Linear Coordination Polymer, Inorg. Chem., 47 (2008) 5218-5224.

[9] N.L. Rosi, J. Eckert, M. Eddaoudi, D.T. Vodak, J. Kim, M. O’Keeffe, O.M. Yaghi, Hydrogen Storage in Microporous Metal-Organic Frameworks, Science 300 (2003) 1127-1129.

[10] B. Moulton, M.J. Zaworotko, From Molecules to Crystal Engineering: Supramolecular Isomerism and Polymorphism in Network Solids, Chem. Rev., 101 (2001) 1629-1658.

[11] a) H.-B. Yang, N. Das, F. Huang, A.M. Hawkridge, D.C. Muddiman, P.J. Stang, Molecular architecture via coordination: self-assembly of nanoscale hexagonal metallodendrimers with designed building blocks**,** J. Am. Chem. Soc., 128 (2006) 10014-10015, and b) C. Janiak, Engineering coordination polymers towards applications, Dalton Trans. (2003) 2781-2804.

[12] G.R. Desiraju, The C−H···O Hydrogen Bond: Structural Implications and Supramolecular Design, Acc. Chem. Res., 29 (1996) 441-449.

[13] a) P. Ghosh, A. R. Chowdhury, S. K. Saha, M. Ghosh, M. Pal, N. C. Murmu, P. Banerjee, Synthesis and characterization of redox non-innocent Cobalt (III) complexes of a O,N,O donor ligand: radical generation, semi-conductivity, antibacterial and anticancer activities, Inorganica Chim. Acta 2015, 429, 99-108; b) S. Ramezani, M. Pordel, A. Davoodnia, Synthesis, characterization and quantum-chemical investigations of new fluorescent heterocyclic Schiff-base ligands and their cobalt(II) complexes, Inorganica Chim. Acta 2019, 484, 450-456; c)) P. Ghosh, A. Roychowdhury, M. Corbella, A. Bhaumik, P. Mitra, S. M. Mobin, A. Mukherjee, S. Basuf, P. Banerjee, Designed synthesis of CO_2-promoted copper(II) coordination polymers: synthesis, structural and spectroscopic characterization, and studies of versatile functional properties, Dalton Trans., 2014, 43, 13500-13508, and d) Y. Thakur, R. Agrawal, M. Tripathi, M. K. Siddiqi, E. Mohapatra, R. H. Khan, R. Pande, Exploring the DNA binding efficacy of Cobalt(II) and Copper(II) complexes of hydroxamic acids and explicating their anti-cancer propensity, J. mol. Str. 2019, 1197, 691-706.

[14] J. Heidebrecht, C. Gendy, B. S. Gelfand, R. Roesler, Water-soluble *NNN*-pincer complexes of cobalt, nickel and palladium: Solid-state structures and catalytic activity, Polyhedron, 143 (2018) 138-143 and references therein.

[15] a) S. M. Soliman, A. El-Faham, One pot synthesis of two Mn(II) perchlorate complexes with *s*-triazine *NNN*-pincer ligand; molecular structure, Hirshfeld analysis and DFT studies, J. Mol. Struct., 1164 (2018) 344-353; b) S. M. Soliman, A. El-Faham, Synthesis, characterization, and structural studies of two heteroleptic Mn(II) complexes with tridentate N,N,N-pincer type ligand, J. Coord. Chem., 71 (2018) 2373-2388.

[16] S. M. Soliman, Z. Almarhoon, E. N. Sholkamy, A. El-Faham, *Bis*-pyrazolyl-*s*-triazine Ni(II) pincer complexes as selective Gram positive antibacterial agents; synthesis, structural and antimicrobial studies, J. Mol. Struct., 1195 (2019) 315-322.

[17] S. M. Soliman, A. El-Faham, Synthesis, X-ray structure, and DFT studies of five- and eight-coordinated Cd(II) complexes with *s*-triazine N-pincer chelate, J. Coord. Chem., 72 (2019) 1621-1636.

[18] S. M. Soliman, Z. Almarhoon, A. El-Faham, Synthesis, Molecular and Supramolecular Structures of New Cd(II) Pincer-Type Complexes with s-Triazine Core Ligand, Crystals, 9 (2019) 226.

[19] S. M. Soliman, J. H. Albering, E. N. Sholkamy, A. El-Faham, Mono- and penta-nuclear self-assembled silver(I) complexes of pyrazolyl *s*-triazine ligand; synthesis, structure and antimicrobial studies, App. Organomet. Chem., 34 (2020) e5603.

[20] A. Sharma, H. Ghabbour, S. T. Khan, G. Beatriz, F. Albericio, A. El-Faham, Novel pyrazolyl-*s*-triazine derivatives, molecular structure and antimicrobial activity, J. Mol. Str., 1145 (2017) 244-253.

[21] S.N. Mikhaylichenko, S.M. Patel, S. Dalili, A. A. Chesnyuk, V.N. Zaplishny, Synthesis and structure of new 1,3,5-triazine-pyrazole derivatives, Tetrahedron Lett., 50 (2009) 2505-2508.

[22] C. Yang, W.-T. Wong, Y. Cui, Y. Yang, Synthesis and crystal structure of nickel(II) and zinc(II) complexes with 2,4-*bis*(3,5-dimethylpyrazol-1-yl)-6-methoxyl-1,3,5-triazine, Science in China Series B: Chemistry, 44 (2001) 80-92.

[23] a) Bruker AXS (2015). SAINT, Version 8.37A, Bruker AXS Inc., Madison, Wisconsin, USA; b) Sheldrick, G. M. *SADABS - Bruker Nonius scaling and absorption correction -*, Bruker AXS, Inc.: Madison, Wisconsin, USA, 2016; c) Sheldrick, G. M. *Acta Cryst.* 2015, *C71*, 3-8.

[24] a) M. J. Turner, J. J. McKinnon, S. K. Wolff, D. J. Grimwood, P. R. Spackman, D. Jayatilaka, M. A. Spackman, Crystal Explorer 17 (2017) University of Western Australia; http://hirshfeldsurface.net; b) F.L. Hirshfeld, Theor. Chim. Acta 44 (1977) 129-138; c) M.A. Spackman, D. Jayatilaka, Cryst. Eng. Comm., 11 (2009) 19-32; d) M.A. Spackman, J.J. McKinnon, Cryst. Eng. Commun., 4 (2002) 378-392; e) J. Bernstein, R.E. Davis, L.

Shimoni, N.-L. Chang, Angew. Chem. Int. Ed., 34 (1995) 1555-1573; f) J.J. McKinnon, D. Jayatilaka, M.A. Spackman, Chem. Comm., (2007) 3814-3816.

[25] a) E.D. Glendening, A.E. Reed, J.E. Carpenter, F. Weinhold, NBO Version 3.1, CI, University of Wisconsin, Madison, (1998), b) M.J. Frisch, G.W. Trucks, H.B. Schlegel, G.E. Scuseria, M.A. Robb, J.R. Cheeseman, G.Scalmani, V.Barone, B.Mennucci, G.A. Petersson, H.Nakatsuji, M. Caricato, X. Li, H.P. Hratchian, A.F. Izmaylov, J.Bloino, G.Zheng, J.L. Sonnenberg, M. Hada, M. Ehara, K. Toyota, R. Fukuda, J. Hasegawa, M. Ishida, T. Nakajima, Y. Honda, O. Kitao, H. Nakai, T. Vreven, J.A. Montgomery, Jr., J.E. Peralta, F. Ogliaro, M. Bearpark, J.J. Heyd, E. Brothers, K.N. Kudin, V.N. Staroverov, R. Kobayashi, J. Normand, K. Raghavachari, A. Rendell, J.C. Burant, S.S. Iyengar, J. Tomasi, M. Cossi, N. Rega, J.M. Millam, M. Klene, J.E. Knox, J.B. Cross, V. Bakken, C. Adamo, J. Jaramillo, R. Gomperts, R.E. Stratmann, O. Yazyev, A.J. Austin, R. Cammi, C. Pomelli, J.W. Ochterski, R.L. Martin, K. Morokuma, V.G. Zakrzewski, G.A. Voth, P. Salvador, J.J. Dannenberg, S. Dapprich, A.D. Daniels, O. Farkas, J.B. Foresman, J.V. Ortiz, J. Cioslowski, D.J. Fox, GAUSSIAN 09. Revision A02. Gaussian Inc., Wallingford CT, USA (2009), and c) GaussView, Version 4.1, R. Dennington II, T. Keith, J. Millam, Semichem Inc., Shawnee Mission, KS, (2007).

[26] a) T. Lu, F. Chen, J. Comp. Chem., **33**, 580 (2012), and b) R. F. W. Bader, Atoms in Molecules: A Quantum Theory, Oxford University Press, Oxford, U.K., 1990.

[27] C. Adamo, V. Barone, Exchange functionals with improved long-range behavior and adiabatic connection methods without adjustable parameters: The mPWmPW and mPW1PWmPW1PW models, J. Chem. Phys., 108 (1998) 664-675.

[28] a) K.M. Ok, P.S. Halasyamani, D. Casanova, M. Llunell, S. Alvarez, Distortions in octahedrally coordinated d^0 transition metal oxides: a continuous symmetry measures approach, Chem. Mater. 18 (2006) 3176-3183; b) A. Santiaqo, A. David, M. Llunell, M. Pinsky, Continuous symmetry maps and shape classification. The case of six-coordinated metal compounds, New J. Chem. 26 (2002) 996-1009; c) Z. Hagit, P. Shmuel, A. David, Continuous symmetry measures, J. Am. Chem. Soc. 114 (1992) 7843-7851; d) http://www.csm.huji.ac.il/new/.

[29] A.W. Addison, T.N. Rao, J. Reedijk, J.V. Rijn, G.C. Verschoor, Synthesis, structure, and spectroscopic properties of copper(II) compounds containing nitrogen–sulphur donor

ligands; the crystal and molecular structure of aqua[1,7-*bis*(*N*-methylbenzimidazol-2′-yl)-2,6-dithiaheptane]copper(II) perchlorate, J. Chem. Soc., Dalton Trans., (1984) 1349-1356.

[30] S.M. Soliman, M.A.M. Abu-Youssef, J. Albering, A. El-Faham, Molecular structure and DFT investigations on new cobalt(II) chloride complex with superbase guanidine type ligand, J. Chem. Sci. 127 (2015) 2137-2149.

[31] C.F. Matta, J. Hernandez-Trujillo, T.-H. Tang, R.F.W. Bader, Hydrogen-hydrogen bonding: a stabilizing interaction in molecules and crystals, Chem. Eur. J. 9 (2003) 1940-1951.

[32] S.J. Grabowski, A. Pfitzner, M. Zabel, A.T. Dubis, M. Palusiak, Intramolecular H…H interactions for the Crystal Structures of [4-((E)-But-1-enyl)-2,6-dimethoxyphenyl]pyridine-3-carboxylate and [4-((E)-Pent-1-enyl)-2,6-dimethoxyphenyl]pyridine-3-carboxylate; DFT calculations on modeled styrene derivatives, J. Phys. Chem. B 108 (2004) 1831-1837.

[33] C.F. Matta, N. Castillo, R.J. Boyd, Characterization of a closed-shell fluorine-fluorine bonding interaction in aromatic compounds on the basis of the electron density, J. Phys. Chem. A 109 (2005) 3669-3681.

[34] A.M. Pendás, E. Francisco, M.A. Blanco, C. Gatti, Bond paths as privileged exchange channels, Chem. Eur. J. 13 (2007) 9362-9371.

[35] M.F. Bobrov, G.V. Popova, V.G. Tsirelson, A topological analysis of electron density and chemical bonding in cyclophosphazenes $P_nN_nX_{2n}$ (X = H, F, Cl; n = 2, 3, 4), Russ. J. Phys. Chem. 80 (2006) 584-590.

[36] C. Gatti, Chemical bonding in crystals: new directions, Z. Kristallogr. 220 (2005) 399-457; (b) G.V. Gibbs, R.T. Downs, D.F. Cox, N.L. Ross, M.B. Boisen Jr., K.M. Rosso, Shared and closed-shell O-O interactions in silicates, J. Phys. Chem. A 112 (2008) 3693-3699.

[37] E. Espinosa, E. Molins, C. Lecomte, Hydrogen bond strengths revealed by topological analyses of experimentally observed electron densities, Chem. Phys. Lett. 285 (1998) 170-173

[38] D. Cremer, E. Kraka, Chemical bonds without bonding electron density-does the difference electron-density analysis suffice for a description of the chemical bond? Angew Chem. Int. Ed. Engl. 23 (1984) 627-628.

Table 5 Spin density of the donor atoms and the central metal ion in complexes **1**, **2A** and **2B**.

Atom	1	2A	2B
Cu/Co	0.5941	2.7342	2.7505
Cl1	0.1470	0.0993	0.0853
Cl2	0.1501	0.0965	0.0867
$\mathbf{N_{triaz.}}$	0.0472	0.0162	0.0242
$\mathbf{N_{pyraz.}}$	0.0498	0.0122	0.0140
O3			0.0084

Table 6 The AIM topological parameters for the studied coordination interactions[a].

Bond	ρ(r)	G(r)	V(r)	E_{int}	H(r)	V(r)/G(r)
			1			
Cu1-N1	0.071	0.094	-0.101	31.841	-0.007	1.079
Cu1-N6	0.065	0.094	-0.098	30.762	-0.004	1.043
Cu1-Cl1	0.058	0.086	-0.089	27.833	-0.003	1.035
Cu1-Cl2	0.050	0.072	-0.071	22.415	0.000	0.994
			2A			
Co1B-N1B	0.088	0.125	-0.148	46.306	-0.023	1.184
Co1B-N6B	0.070	0.089	-0.101	31.558	-0.012	1.131
Cu1-Cl1	0.074	0.100	-0.117	36.698	-0.017	1.173
Cu1-Cl2	0.066	0.088	-0.099	31.142	-0.011	1.128
			2B			
Co1-N1	0.083	0.120	-0.140	43.908	-0.020	1.168
Co1-N6	0.045	0.051	-0.052	16.366	-0.001	1.028
Co1-Cl1	0.055	0.070	-0.075	23.514	-0.005	1.075
Co1-Cl2	0.062	0.081	-0.089	28.049	-0.009	1.107
Co1-O3	0.043	0.063	-0.066	20.564	-0.003	1.046

[a] All in A.U. except $E_{int.}$ in kcal/mol

Highlights

- Monopyrazolyl-*s*-triazine (**PTM**) complexes with Co(II) and Cu(II) were synthesized
- **PTM** acts as a bidentate *NN*-chelating ligand
- **1** and **2A** have a distorted tetrahedral [M(PTM)Cl_2] coordination environment.
- [Co(PTM)Cl_2(EtOH)]; **2B** is highly distorted penta-coordinated Co(II) complex.
- The H…H (49.0-55.1%), Cl…H (18.8-20.5%) and O…H (8.3-9.9%) are the most important contacts.

Dear editor in chief of "**Journal of Molecular Structure**"

Dear Sir,

We would like to submit the paper entitled "Molecular and supramolecular structures of self-assembled Cu(II) and Co(II) complexes with 4,4'-[6-(3,5-dimethyl-1*H*-pyrazol-1-yl)-1,3,5-triazine-2,4-diyl]dimorpholine ligand" to your journal "**Journal of Molecular Structure**"

The authors declare that they have no known competing financial interests or personal relationships that could have appeared to influence the work reported in this paper.

Thank you

Saied M Soliman

Faculty of Science, Alexandria University, P.O. Box 426 Ibrahimia, , 21321 Alexandria, Egypt